

A new type of instability: explosive disturbances in a liquid film inside a rotating horizontal cylinder

By E. S. BENILOV¹, S. B. G. O'BRIEN¹ AND I. A. SAZONOV^{2†}

¹Department of Mathematics, University of Limerick, Ireland

²Department of Applied Mathematics, University College Cork, Ireland

(Received 5 August 2002 and in revised form 2 December 2002)

We examine the dynamics of a thin film of viscous fluid on the inside surface of a cylinder with horizontal axis, rotating around this axis. An asymptotic equation is derived, which takes into account two orders of the so-called lubrication approximation. The equation admits a solution describing a steady-state distribution of film around the cylinder, and we examine the stability of this solution. It is demonstrated that the linearized problem admits infinitely many harmonic solutions, all of which have real frequencies (are neutrally stable). On the other hand, there are non-harmonic solutions that ‘explode’ (develop singularities) in a finite time. Systems having solutions of both types simultaneously have never been described in the literature. An example of this phenomenon is the main result of this paper.

1. Introduction

Disturbances with harmonic dependence on time play an important role in linear stability analysis (e.g. Drazin & Reid 1981). For unstable systems, they provide a simple growing solution and thus help to prove instability. On the other hand, systems with an infinite set of bounded harmonic disturbances are usually regarded as proved stable. In such cases, the initial condition can be represented by a series of disturbances and, since these are stable, so is every solution. Even systems with a finite set of bounded harmonic disturbances (and no growing ones) are often regarded as stable. Although no such theorem can be proved, of course, exceptions are few and are mostly restricted to systems with two or more coinciding harmonic frequencies, in which case algebraically growing (non-harmonic) solutions may exist. Apart from these, there also exist systems with so-called ‘transient’ (again, non-harmonic) disturbances, which initially grow, and sometimes quite significantly, but always eventually decay, or rather disperse (e.g. Farrel 1982; Trefethen *et al.* 1993; Sazonov 1996; Chapman 2002).

In the present paper, a (hydrodynamic) system will be presented, which supports infinitely many bounded harmonic disturbances. Yet, the system is unstable, and the instability is strong, as there are disturbances that blow up in a finite time. Such disturbances are uncharacteristic of linear systems and are similar to solutions

† Present address: School of Engineering, University of Wales Swansea, Singleton Park, Swansea, SA2 8PP, UK.

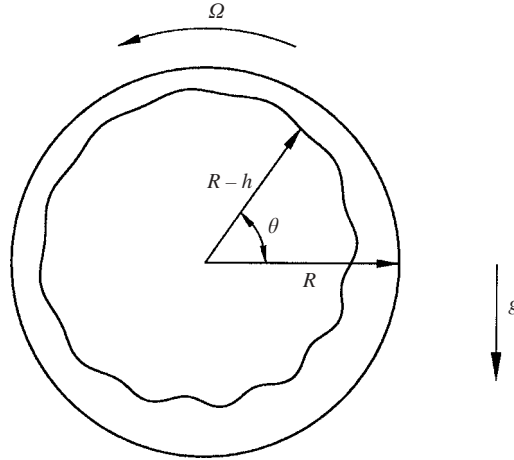


FIGURE 1. Formulation of the problem: film in a rotating cylinder with horizontal axis.

describing the so-called ‘explosive’ instability in nonlinear media (see Blombergen 1965 and references therein).

The paper has the following structure: in §2, we describe the physical setting where the new instability will be examined – a thin liquid film on the inside surface of a rotating cylinder. Two models governing the film are considered: a general asymptotic equation based on the so-called lubrication approximation, and its simplified version (obtained for the limit of small mass flux). Using the latter, we examine harmonic (§3) and non-harmonic (§4) disturbances. In §5, we generalize our conclusions for the ‘full’ (non-simplified) equation.

2. Formulation

Consider a thin film of liquid on the inside surface of a cylinder of radius R , with a horizontal axis, which is rotating about this axis with constant angular velocity Ω (see figure 1). We use polar coordinates (r, θ) , with the origin at the centre of the cylinder, so the thickness h of the film depends on θ and the time t .

In addition to R , the problem includes another characteristic length. To introduce it, observe that the volume of fluid per unit length of cylinder,

$$\int_0^{2\pi} \int_{R-h}^R r \, dr \, d\theta = \int_0^{2\pi} (Rh - \frac{1}{2}h^2) \, d\theta,$$

is conserved. Then, we can define

$$l = \frac{1}{2\pi R} \int_0^{2\pi} (Rh - \frac{1}{2}h^2) \, d\theta.$$

If $h \ll R$ (which is the limit we are interested in), l represents the mean thickness of the film.

The evolution of the film is governed by three non-dimensional parameters. First, we introduce the mean relative thickness,

$$\delta = \frac{l}{R}. \quad (2.1)$$

Secondly, we define the ratio of the gravitational and centrifugal forces,

$$G = \frac{g}{\Omega^2 R}, \quad (2.2)$$

where g is the acceleration due to gravity. Finally, we introduce a parameter characterizing viscosity (again, relative to the rotation),

$$N = \frac{\nu}{\Omega l^2}, \quad (2.3)$$

where ν is the kinematic viscosity.

The so-called lubrication approximation assumes that

$$\begin{aligned} \delta &\ll 1, \\ G &\sim N \gg 1, \end{aligned} \quad (2.4)$$

which implies that gravity and viscosity are of the same order, and are much stronger than inertia. Using these assumptions, a relatively simple asymptotic equation can be derived (see Moffat 1977; Johnson 1988). Introducing the following non-dimensional variables,

$$\hat{t} = \Omega t, \quad \hat{h} = \sqrt{\frac{g}{\nu \Omega R}} h,$$

and omitting the hats, we can write down this equation in the form

$$\frac{\partial h}{\partial t} + \frac{\partial}{\partial \theta} \left(h - \frac{1}{3} h^3 \cos \theta \right) = 0. \quad (2.5)$$

For a steady-state solution,

$$h(\theta, t) = \bar{h}(\theta),$$

(2.5) yields

$$\bar{h} - \frac{1}{3} \bar{h}^3 \cos \theta = q, \quad (2.6)$$

where q is a constant of integration (physically, q is the non-dimensional mass flux). It has been demonstrated (Johnson 1988) that equation (2.6) has a smooth unique solution for $0 < q < 2/3$, describing a steady-state flow[†] (examples of these solutions are shown in figure 2).

The stability properties of equation (2.5) have been examined by O'Brien (2002a): $\bar{h}(\theta)$ turned out to be neutrally stable. Given that (2.5) is a leading-order approximation, this result is not indicative of the stability of the exact model, as the higher-order corrections may affect the stability of $\bar{h}(\theta)$ either way. For example, O'Brien (2002b) demonstrated that weak capillary effects, if taken into account in a similar problem, can make the flow asymptotically stable, though the numerics of this paper suggested that anti-diffusion effects always give rise to unstable normal modes.

In the present paper, we examine the effect of the higher-order terms of the lubrication approximation on the stability of the steady solution $\bar{h}(\theta)$. For simplicity, the effect of inertia is ignored, which implies

$$G \sim N \gg \delta^{-1} \quad (2.7)$$

(observe that (2.7) is marginally stronger than condition (2.4)). Following a straightforward asymptotic expansion (see Appendix A), we obtain the following higher-order

[†] If $q = 2/3$, (2.6) also admits a shock-wave type solution (see Johnson 1988; O'Brien & Gath 1988). Such solutions will not be considered in this paper.

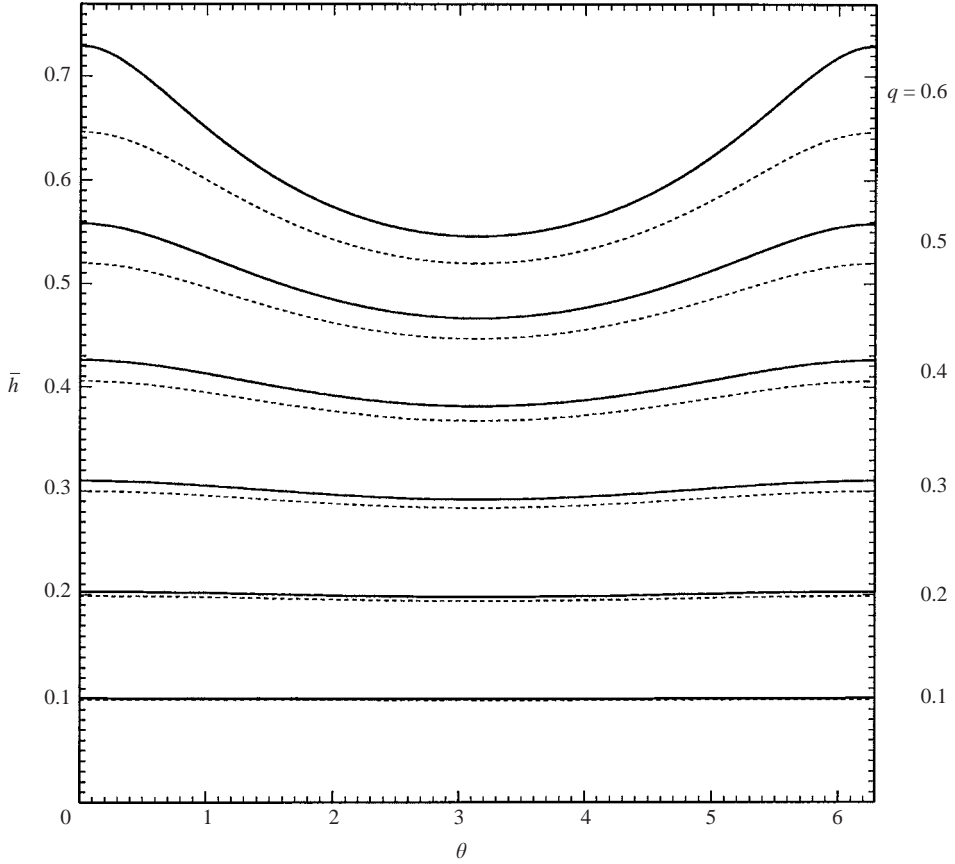


FIGURE 2. Steady-state flow of the film for various values of the flux q . The solid line shows the solution of the zeroth-order equation (2.6), the dotted line shows the asymptotic solution (2.10) of the first-order equation.

analogues of (2.5) and (2.6)

$$(1 - \varepsilon h) \frac{\partial h}{\partial t} + \frac{\partial}{\partial \theta} \left[h - \frac{1}{3} h^3 \cos \theta + \varepsilon \left(\frac{1}{2} h^4 \cos \theta + \frac{1}{3} h^3 \frac{\partial h}{\partial \theta} \sin \theta - \frac{1}{2} h^2 \right) \right] = 0, \quad (2.8)$$

$$\bar{h} - \frac{1}{3} \bar{h}^3 \cos \theta + \varepsilon \left(\frac{1}{2} \bar{h}^4 \cos \theta + \frac{1}{3} \bar{h}^3 \frac{d\bar{h}}{d\theta} \sin \theta - \frac{1}{2} \bar{h}^2 \right) = q, \quad (2.9)$$

where

$$\varepsilon = \delta \sqrt{\frac{N}{G}} = \sqrt{\frac{\nu \Omega}{gR}}$$

is a small parameter comparable to δ . Equation (2.9) can be solved using a simple perturbation technique based on the smallness of ε ,

$$\bar{h} = \bar{h}^{(0)} - \frac{\varepsilon \left(\frac{1}{2} \bar{h}^{(0)4} \cos \theta + \frac{1}{3} \bar{h}^{(0)3} \frac{d\bar{h}^{(0)}}{d\theta} \sin \theta - \frac{1}{2} \bar{h}^{(0)2} \right)}{1 - h^{(0)2} \cos \theta} + O(\varepsilon^2), \quad (2.10)$$

where $\bar{h}^{(0)}$ is the solution of the leading-order equation (2.6). In fact, figure 2 shows that, provided ε is small and q is not close to $2/3$, \bar{h} does not differ much from its leading-order approximation.

In what follows, the evolution equation (2.8) will be used to examine the stability of \bar{h} with respect to small disturbances. Assuming that

$$h(\theta, t) = \bar{h}(\theta) + h'(\theta, t),$$

where h' describes a disturbance, we substitute $h(\theta, t)$ into (2.8) and omit the nonlinear terms. Dropping the primes, we obtain

$$B(\theta) \frac{\partial h}{\partial t} + \frac{\partial}{\partial \theta} \left[C(\theta) h + \varepsilon D(\theta) \sin \theta \frac{\partial h}{\partial \theta} \right] = 0, \tag{2.11}$$

where

$$B = 1 - \varepsilon \bar{h}, \quad C = 1 - \bar{h}^2 \cos \theta + \varepsilon \left(2\bar{h}^3 \cos \theta + \bar{h}^2 \frac{d\bar{h}}{d\theta} \sin \theta - \bar{h} \right), \quad D = \frac{1}{3} \bar{h}^3. \tag{2.12}$$

Equation (2.11) describes propagation and diffusion of disturbances (the first and second terms in the square brackets, respectively). The expression

$$-\varepsilon D(\theta) \sin \theta$$

is the effective diffusivity coefficient. Observe that, in the lower half of the cylinder ($-\pi < \theta < 0$), the diffusivity is positive, whereas in the upper half ($0 < \theta < \pi$), it is negative. The *sign-variable* diffusivity makes equation (2.11) special and has far-reaching implications. First, the region of negative diffusivity makes most numerical schemes (both pseudospectral and finite-difference) unstable and makes it extremely difficult to simulate (2.11) numerically. Secondly, the variable diffusivity, together with all other coefficients being variable, hampers the use of analytical methods. Thus, for the sake of simplicity, we examine (2.11) in two steps. We start from the small-flux limit, $q \rightarrow 0$. In this case, $\bar{h}(\theta)$ becomes flat (see figure 2) and equation (2.9) yields

$$\bar{h}(\theta) = q + O(q^3, \varepsilon q^2) \quad \text{as } q \rightarrow 0$$

(this approximation, in fact, works well both for small and moderate q – see figure 2). Accordingly, the coefficients of equation (2.11) are close to constants,

$$B = 1 + O(\varepsilon q), \quad C = 1 + O(q^2, \varepsilon q), \quad D = \frac{1}{3} q^3 + O(q^5, \varepsilon q^4) \quad \text{as } q \rightarrow 0,$$

and (2.11) tends to

$$\frac{\partial h}{\partial t} + \frac{\partial}{\partial \theta} \left(h + \varepsilon \sin \theta \frac{\partial h}{\partial \theta} \right) = 0, \tag{2.13}$$

where

$$\varepsilon = \frac{1}{3} \varepsilon q^3.$$

We note that, when deriving (2.13), we have omitted terms $O(q^2)$ (from C) and retained terms $O(\varepsilon q^3)$ (in εD). Observe, however, that the latter is multiplied by the second derivative of h' , whereas the former is multiplied by the first derivative – hence, we can rescale θ to make the above approximation consistent. Alternatively, we can just look at equation (2.13) as a simple qualitative model of sign-variable diffusivity – having understood the general dynamics of such systems, we shall re-examine the exact equation (2.11).

3. The small- q limit: harmonic disturbances

In this section, we shall examine the harmonic solutions of equation (2.13), i.e. solutions of the form

$$h(\theta, t) = \phi(\theta)e^{-i\omega t}. \quad (3.1)$$

Substitution of (3.1) into (2.13) yields an o.d.e. for $\phi(\theta)$,

$$\epsilon \sin \theta \frac{d^2 \phi}{d\theta^2} + (1 + \epsilon \cos \theta) \frac{d\phi}{d\theta} - i\omega \phi = 0. \quad (3.2)$$

This equation and the periodicity condition,

$$\phi(0) = \phi(2\pi), \quad (3.3)$$

form an eigenvalue problem for ϕ and ω . If $\text{Im } \omega > 0$, the film is unstable.

Observe that $\theta = 0$ and $\theta = \pi$ are singular points of equation (3.2), as the coefficient of the highest-order derivative at these points vanish. Interestingly, they do not cause singular behaviour of the solution (see Appendix B) and we can assume $\phi(\theta)$ is continuous.

Equation (3.2) contains a small parameter, ϵ , which enables us to solve (3.2) using a suitable asymptotic method. The simplest of such is the straightforward expansion in powers of ϵ , i.e.

$$\phi = \phi^{(0)} + \epsilon \phi^{(1)} + \dots, \quad \omega = \omega^{(0)} + \epsilon \omega^{(1)} + \dots \quad (3.4)$$

Substituting (3.4) into (3.2) and solving for $\phi^{(0)}$, $\phi^{(1)}$... (details omitted), we find a countable set of modes

$$\phi = e^{in\theta} - \epsilon n e^{2in\theta} + \frac{3}{2} \epsilon^2 n^2 e^{3in\theta} + \dots, \quad (3.5)$$

$$\omega = n + \epsilon^2 n^3 + \dots, \quad (3.6)$$

where $n = 0, \pm 1, \pm 2, \dots$ is the mode number. Observe that all eigenvalues are real (neutrally stable).

Note, however, that solution (3.5)–(3.6) does not work very well for modes with large n , as the correction terms (the second/third terms in (3.5), and the second term in (3.6)) grow in the limit $n \rightarrow \infty$, $\epsilon = \text{const}$. This conclusion agrees with the numerical solution of the eigenvalue problem (3.2), (3.3) – see figure 3 (the numerical method is described in Appendix C).

In order to find a solution applicable for large ω (higher modes), we use a modification of the WKB method. First, we introduce λ such that

$$\omega = \frac{\lambda}{\epsilon} \quad (3.7)$$

and then seek a solution of the form

$$\phi(\theta) = \exp \left[\frac{1}{\epsilon} \int_0^\theta S(\theta') d\theta' \right], \quad (3.8)$$

where $S(\theta)$ is the new unknown function. Substitution of (3.7)–(3.8) into (3.2) yields

$$S^2 \sin \theta + S - i\lambda + \epsilon \left(S \cos \theta + \frac{dS}{d\theta} \sin \theta \right) = 0.$$

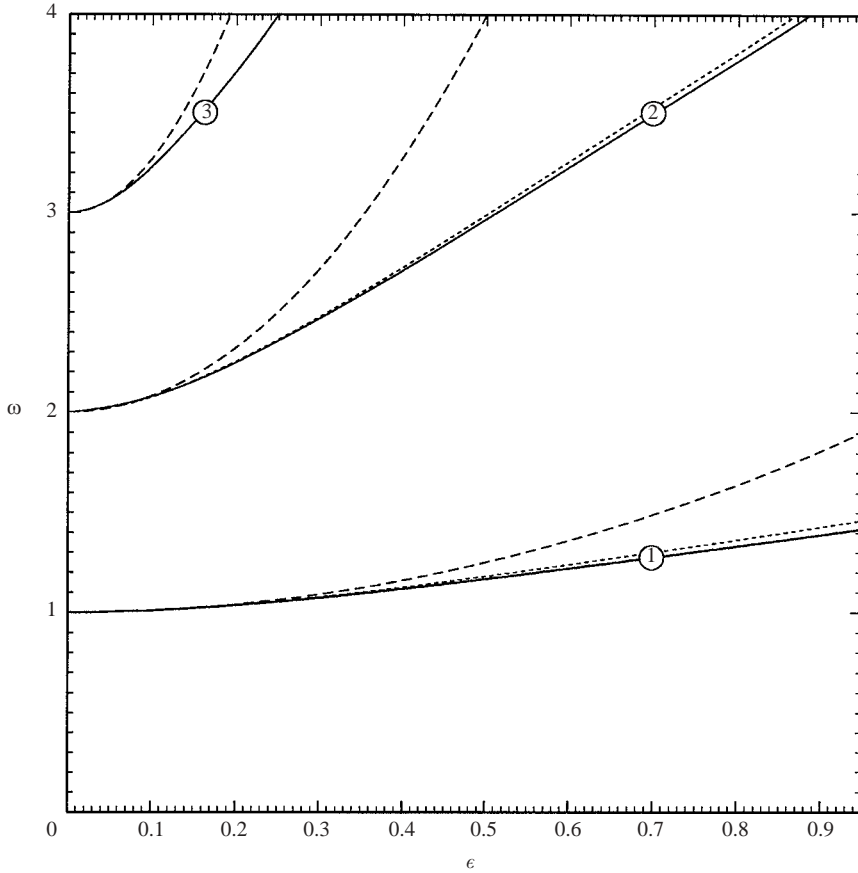


FIGURE 3. The eigenvalues of problem (3.2), (3.3) vs. ϵ , for the first three modes. The curves are marked with the mode number. The solid line shows the exact solution (computed numerically), the dashed line shows the straightforward expansion in ϵ (equation (3.6)), and the dotted line shows the WKB solution (equation (3.10)). For the third mode, the WKB solution is indistinguishable from the exact one.

Expanding S in powers of ϵ ,

$$S = S_0 + \epsilon S_1 + \dots,$$

we can readily obtain,

$$S_0^2 \sin \theta + S_0 - i\lambda = 0.$$

This (quadratic) equation has two solution for S_0 , one of which is singular at $\theta = 0$ and, hence, should be discarded. The other one is

$$S_0 = \frac{\sqrt{1 + 4i\lambda \sin \theta} - 1}{2 \sin \theta},$$

where the branch of the square-root function is chosen such that $\sqrt{1} = 1$. The equation for S_1 ,

$$2S_0 S_1 \sin \theta + S_1 + S_0 \cos \theta + \frac{dS_0}{d\theta} \sin \theta = 0,$$

can also be readily solved,

$$S_1 = -\frac{i\lambda}{1 + 4i\lambda \sin \theta} \cos \theta.$$

Substituting the expressions for S_0 and S_1 into (3.8), solving the integral of S_1 , and substituting ω for λ (see (3.7)), we obtain

$$\phi = \frac{1}{(1 + 4i\epsilon\omega \sin \theta)^{1/4}} \exp \left(\int_0^\theta \frac{\sqrt{1 + 4i\epsilon\omega \sin \theta'} - 1}{2\epsilon \sin \theta'} d\theta' \right). \tag{3.9}$$

Clearly, (3.9) is periodic when

$$\int_0^{2\pi} \frac{\sqrt{1 + 4i\epsilon\omega \sin \theta} - 1}{2\epsilon \sin \theta} d\theta = 2\pi i n, \tag{3.10}$$

where, as before, n is the mode number. This equation determines the eigenvalue ω , and can be rewritten in a more convenient form by subdividing the region of integration into two parts $[(-\pi, 0)$ and $(0, \pi)]$, replacing θ with $-\theta$ in the former, and reducing the latter to $(0, \pi/2)$. Straightforward algebra yields an equation

$$f(\omega) = n, \tag{3.11}$$

where

$$f(\omega) = \int_0^{\pi/2} \frac{\sqrt{1 + 4i\epsilon\omega \sin \theta} - \sqrt{1 - 4i\epsilon\omega \sin \theta}}{2\pi i \epsilon \sin \theta} d\theta.$$

It can be readily shown that the function $f(\omega)$ has the following properties:

- (i) If $\text{Im } \omega \neq 0$, then $\text{Im } f(\omega) \neq 0$. Hence, (3.11) does not have complex roots.
- (ii) For real ω , $f(\omega)$ is a real monotonically growing function, such that

$$\begin{aligned} f(\omega) &= 0 && \text{if } \omega = 0, \\ f(\omega) &\rightarrow \infty && \text{as } \omega \rightarrow \infty. \end{aligned}$$

Hence, for any n , (3.11) has a unique real root $\omega = \omega_n$.

We conclude that harmonic solutions of the evolution equation (2.13) are neutrally stable up to two orders of the WKB expansion.

Note that, if $\epsilon\omega_n \ll 1$, (3.11) yields $\omega_n \approx n + \epsilon^2 n^3$, which agrees with the straightforward expansion in ϵ (see (3.6)). Thus, the WKB method is, in fact, applicable to both high and low modes (the latter was not expected). In the opposite limit, $\epsilon\omega_n \gg 1$, (3.11) can also be solved asymptotically (details omitted), but in the general case, it has to be solved numerically (using Simpson's rule and the secant method). We have done so, and we compared the computed values of ω to the numerical solution of the original (exact) eigenvalue problem (3.2), (3.3). Typical results are given in table 1.

For the lowest modes, the WKB results coincide with those of the straightforward expansion in ϵ , and the error of the latter is $O(\epsilon^4)$. At the same time, the accuracy of the WKB method should improve with growing mode number. The maximum error occurs somewhere in the range $\omega \sim \epsilon^{-1}$, and the error itself is $O(\epsilon^2)$ (recall that we have taken into account two orders of the WKB expansion). For $\epsilon = 0.1$, for example, the maximum error occurs for the 15th mode.

We have also compared the asymptotic eigenfunctions (given by (3.9)) with the exact (computed) ones. In all cases, the difference was so small that the two graphs are virtually indistinguishable, even for the 15th mode. Typical behaviour of the eigenfunctions is shown in figure 4. We can see that the maximum of the mode's

Mode number	Eigenvalues (numerical)	Eigenvalues (WKB)	Relative error
1	1.0097	1.0098	0.01%
2	2.0733	2.0739	0.03%
3	3.2297	3.2311	0.04%
4	4.5012	4.5034	0.05%
5	5.8992	5.9026	0.06%
6	7.4298	7.4351	0.07%
7	9.0951	9.1045	0.10%
8	10.8945	10.9130	0.17%
9	12.8252	12.8619	0.29%
10	14.8820	14.9521	0.47%
...
15	27.1631	27.538	1.38%
...
20	44.0170	43.6990	0.72%

TABLE 1. The comparison of the exact (numerical) eigenvalues ω_n of problem (3.2), (3.3), to those obtained asymptotically through (3.11) (WKB method), for $\epsilon = 0.1$.

amplitude occurs at $\theta = \pi$, which can be interpreted as follows: the disturbance sets out from $\theta = 0$ with unit amplitude and grows, travelling through the top half of the cylinder, $0 < \theta < \pi$. In the bottom half of the cylinder it decays and, having reached $\theta = 2\pi$, restores its initial amplitude. This process can conveniently be characterized by an ‘amplification coefficient’

$$A_n = \frac{|\phi_n(\pi)|}{|\phi_n(0)|}.$$

Having in mind the (high) accuracy of the WKB method, we shall calculate A_n using this approximation,

$$A_n = \exp \left(\operatorname{Re} \int_0^\pi \frac{\sqrt{1 + 4i\epsilon\omega_n \sin \theta} - 1}{2\epsilon \sin \theta} d\theta \right). \tag{3.12}$$

The WKB values of A_n are given in table 2. We can see that A_n rapidly grows with the mode number. This growth makes higher-order modes extremely difficult to compute and makes the WKB method the only tool for obtaining the eigenfunctions.

Finally, we note that eigenfunctions with $n = O(\epsilon^{-1})$ oscillate in θ on the scale of ϵ and thus violate the lubrication approximation (in particular, for such modes the first-order terms in equation (3.2) become comparable to the zero-order terms). However, even though such eigenfunctions have no physical meaning, they are still important mathematically for expanding the solution in a series in harmonic modes (when solving the initial-value problem).

4. The small- q limit: An ‘exploding’ solution

In the previous section, we demonstrated that the evolution equation (2.13) has infinitely many (asymptotic) solutions of the form $\phi_n(\theta) \exp(-i\omega_n t)$. All these solutions are stable, i.e. $\operatorname{Im} \omega_n = 0$ for all n .

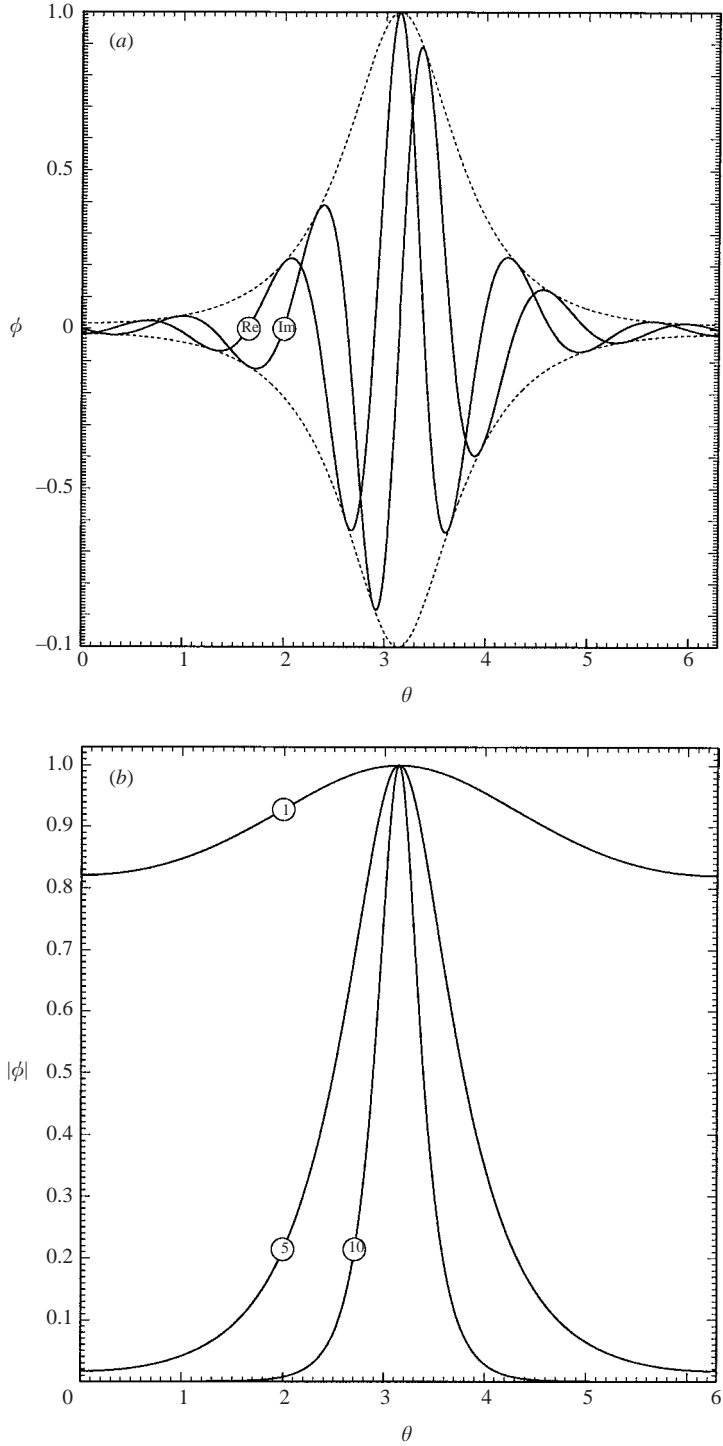


FIGURE 4. Eigenfunctions of problem (3.2), (3.3), for $\epsilon = 0.1$ (the WKB solutions are not shown, as they are indistinguishable from the exact ones). (a) The real and imaginary parts of the eigenfunction of mode 5. The dotted line shows the absolute value of the eigenfunction. (b) The absolute values of the eigenfunctions of modes 1, 5 and 10.

Mode number	Amplification coefficient
1	1.22
2	2.14
3	5.14
4	15.8
5	59.4
6	262
7	1329
8	7535
9	47071
10	319871
...	...
15	1.20037×10^{10}
...	...
20	1.33893×10^{15}

TABLE 2. The amplification coefficient A_n (see (3.12)) calculated using the WKB approximation, for $\epsilon = 0.1$.

In what follows, we assume that the set of eigenfunctions $\{\phi_n, n = 0, \pm 1, \pm 2, \dots\}$ is complete†, and an arbitrary initial condition can be represented by a series

$$h(\theta, 0) = \sum_{n=-\infty}^{\infty} m_n \phi_n(\theta),$$

where m_n are the equivalent of the coefficients of the complex Fourier series. Then, the solution for $t > 0$ is

$$h(\theta, t) = \sum_{n=-\infty}^{\infty} m_n \phi_n(\theta) \exp(-i\omega_n t). \tag{4.1}$$

Since this series converges for $t = 0$ (to the initial condition) and every term is bounded for all $t > 0$, it is natural to assume that (4.1) is bounded for all $t > 0$.

The above argument, however, contains a ‘hole’, as the coefficients of the series depend on t and, even though the series converges at $t = 0$, it may diverge later. Such cases have never been described in the literature, and they are probably extremely rare, but this appears to be the only possible explanation of the ‘exploding’ solution presented below.

4.1. The exploding solution

In this subsection, we present an explicit asymptotic solution, which is unstable regardless of the fact that all harmonic solutions are stable.

Observe that, to the leading order, equation (2.13) yields

$$\frac{\partial h}{\partial t} + \frac{\partial h}{\partial \theta} \approx 0,$$

† Unfortunately, the formal proof of completeness of the set of ϕ_n turned out to be a difficult task (mainly because the corresponding Sturm–Liouville operator is singular). Given the physical nature of this paper, we have ‘verified’ the completeness by expanding various functions in ϕ_n and making sure that truncation error decreases with the growing number of modes taken into account. Observe also that $\phi_n \rightarrow e^{in\theta}$ as $\epsilon \rightarrow 0$, i.e. ϕ_n tend to exponential functions which do form a complete set. This fact is another indirect indication of completeness of the set of ϕ_n .

which means that the solution is translating along the inner surface of the cylinder at a unit speed, in the counterclockwise direction. This suggests changing to a co-moving reference frame, i.e. replacing θ with a new coordinate, say, $y = \theta - t$. In this case, (2.13) becomes:

$$\frac{\partial h}{\partial t} + \epsilon \frac{\partial}{\partial y} \left[\sin(t + y) \frac{\partial h}{\partial y} \right] = 0. \quad (4.2)$$

We seek a narrow pulse-like solution, located at $y = 0$. Accordingly, the 'outer' solution is $h(y, t) = 0$. In the immediate vicinity of the pulse, on the other hand, we use a boundary-layer re-scaling to reflect the increased importance of the spatial derivatives:

$$x = \frac{y}{\sqrt{\epsilon}}, \quad (4.3)$$

where $\sqrt{\epsilon}$ is the boundary-layer thickness. Rewriting (4.2) in terms of (x, t) , we obtain

$$\frac{\partial h}{\partial t} + \frac{\partial}{\partial x} \left[\sin(t + \sqrt{\epsilon}x) \frac{\partial h}{\partial x} \right] = 0.$$

The small parameter in front of x reflects the assumption that the pulse is narrow, and the change of the diffusivity over its width is negligible. Hence, the leading-order 'inner' equation is

$$\frac{\partial h}{\partial t} = -\sin t \frac{\partial^2 h}{\partial x^2}. \quad (4.4)$$

Equation (4.4) is a diffusion equation with variable diffusivity (represented by $-\sin t$). Observe that the diffusivity now depends on the time variable (since the perturbation translates at a unit speed, the coordinate where it is located approximately coincides with t).

It can be verified by inspection that (4.4) admits the following particular solution:

$$h(x, t) = \frac{P}{\sqrt{Q - 4 \sin^2(\frac{1}{2}t)}} \exp \left\{ -\frac{x^2}{2 [Q - 4 \sin^2(\frac{1}{2}t)]} \right\}, \quad (4.5)$$

where P and Q are arbitrary constants. We note that (4.5) matches automatically with the outer solution $h = 0$, i.e. it is actually a composite solution valid on the whole domain.

In order to clarify the physical meaning of solution (4.5), we return to the 'physical' variables (θ, t) and rewrite (4.5) in the form

$$h(\theta, t) = A(t) \exp \left[-\frac{(\theta - t)^2}{2W^2(t)} \right], \quad (4.6)$$

$$A(t) = \frac{A_0 W_0}{\sqrt{W_0^2 - 4\epsilon \sin^2(\frac{1}{2}t)}}, \quad (4.7)$$

$$W(t) = \sqrt{W_0^2 - 4\epsilon \sin^2(\frac{1}{2}t)}, \quad (4.8)$$

where the constants A_0 and W_0 are given by

$$W_0 = \sqrt{\epsilon Q}, \quad A_0 = \frac{P}{\sqrt{Q}}.$$

Solution (4.6)–(4.8) describes a Gaussian pulse, initially positioned at $\theta = 0$. For $t > 0$, it is translating along the inner surface of the cylinder in the counterclockwise direction. The speed of translation is constant (equal to unity), but the amplitude $A(t)$ and width $W(t)$ depend on the pulse’s current position. The constants W_0 and A_0 represent the initial values of $W(t)$ and $A(t)$.

The evolution of the pulse depends on whether W_0 exceeds the threshold value of $2\sqrt{\epsilon}$.

If $W_0 > 2\sqrt{\epsilon}$, solution (4.6)–(4.8) is smooth for all values of t and θ . Between $t = 0$ and $t = \pi$, the pulse is travelling through the upper half of the cylinder, where the diffusivity is negative. Accordingly, the width of the pulse is decreasing and the amplitude is growing. At $t = \pi$, the pulse enters the region of positive diffusivity, and by the time it reaches the starting point ($t = 2\pi$), it restores its initial parameters. This cycle is repeated indefinitely.

If $W_0 \leq 2\sqrt{\epsilon}$, we can see that

$$A(t) \rightarrow \infty \quad \text{as } t \rightarrow t_*,$$

where

$$t_* = 2 \arcsin \left(\frac{W_0}{2\sqrt{\epsilon}} \right)$$

is the time of ‘explosion’ (see figure 5*b*). Thus, if initially the pulse is sufficiently narrow, it blows up before it leaves the upper half of the cylinder owing to the effect of ‘anti-diffusivity’. This is the main result of this section.

Finally, observe that solution (4.6)–(4.8) is not periodic in θ . This shortcoming can be remedied by straightforward ‘periodization’ of (4.6),

$$h(\theta, s) = \sum_{j=-\infty}^{\infty} A(t) \exp \left[-\frac{(t - \theta + 2\pi j)^2}{2W^2(t)} \right]. \tag{4.9}$$

It can be readily demonstrated that, if $W(t) \neq 0$, the series (4.9) converges for all θ , and our conclusions remain intact. Moreover, owing to the fast decay of the Gaussian function with distance, there is little ‘overlapping’ between neighbouring pulses – which means that figure 5 also remains essentially the same.

4.2. Discussion

(i) When dealing with a short-wave asymptotic solution, the main danger is to ‘exceed’ the applicability of the model from which it was obtained. In the present context, solution (4.6)–(4.8) was obtained as a result of a two-step asymptotic procedure: first, we used the lubrication (long-wave) approximation to reduce the equations of fluid dynamics to (2.13); secondly, we assumed the solution to be short-wave and reduced (2.13) to (4.4).

There is, clearly, nothing wrong with the second link of our asymptotic ‘chain’, as the short-wave approximation is actually improving when the pulse is approaching explosion. The situation with the lubrication approximation is somewhat less clear.

In order to clarify whether solution (4.6)–(4.8) is consistent with the lubrication approximation, we assume that the asymptotic equation (2.13) is valid until the zeroth-order terms in it exceed the first-order terms,

$$\left| \frac{\partial h}{\partial \theta} \right| \gg \left| \epsilon \frac{\partial}{\partial \theta} \left(\sin \theta \frac{\partial h}{\partial \theta} \right) \right|.$$

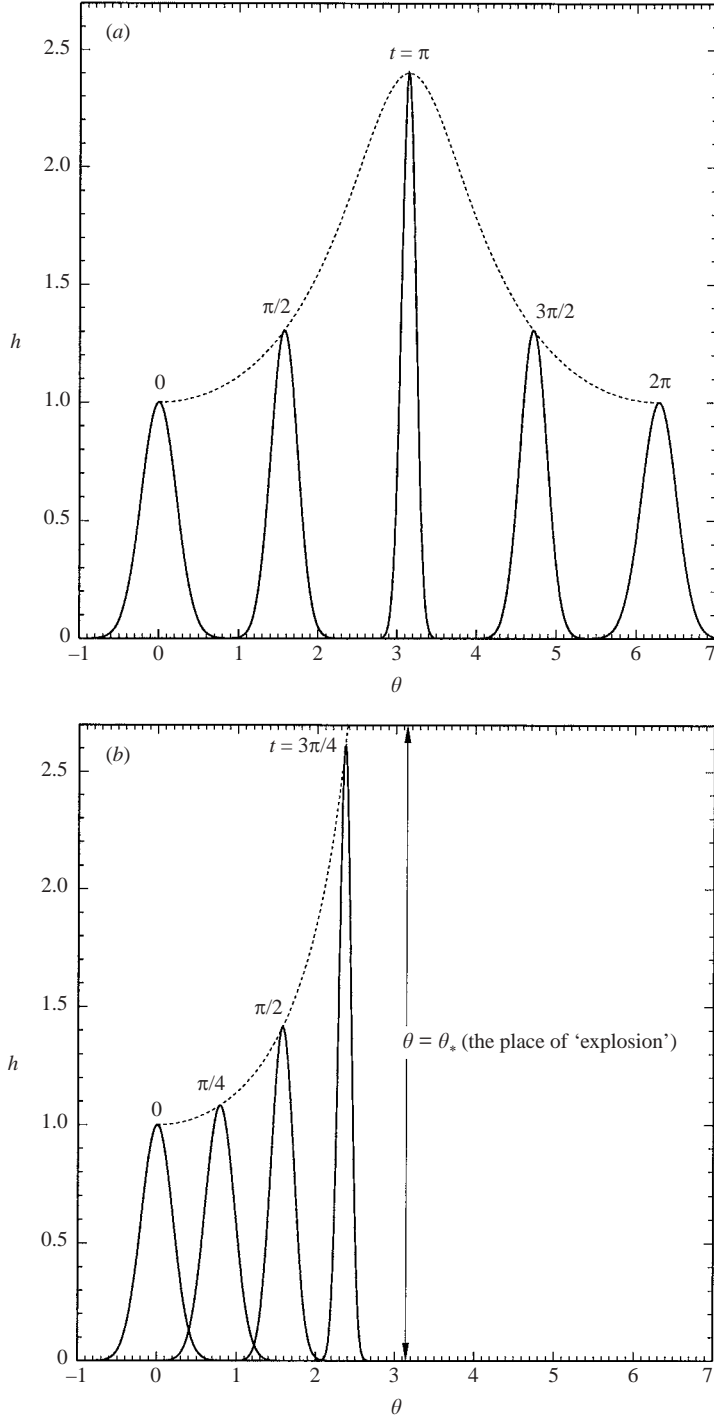


FIGURE 5. The evolution of a Gaussian pulse (solution (4.6a-c)) for $\epsilon = 0.01$. The dotted line shows $A(\theta)$ (see (4.7b)) i.e. the amplitude of the pulse when it reaches the point θ . (a) $W_0 = 0.22$ (a non-exploding case). (b) $W_0 = 0.2$ (an exploding case). The time and place of explosion are both equal to π .

Then we substitute (4.6)–(4.8) into this inequality and obtain a restriction for the width of the pulse,

$$W(t) \gg \epsilon. \tag{4.10}$$

This condition does not restrict the non-exploding asymptotic solutions, the width of which is comparable to its initial value, and the latter is $W_0 \geq O(\sqrt{\epsilon})$, but the exploding solutions can be trusted only until they become narrower than what is allowed by (4.10). This certainly does not cover the time of explosion.

Yet, there is a physical argument which leads us to believe that the exact system also has some kind of singular solutions. Imagine a short-scale perturbation on the surface of the film. When the rotation of the cylinder turns it ‘upside down’, gravity starts increasing its amplitude and/or shortening its size. Once the perturbation is sufficiently large and short, a drop of fluid should detach itself from the film and start falling down. Clearly, the exploding solution of the linear asymptotic equation describes the initial stage of this process, and, unless capillary effects are taken into account, the exact model should admit a similar solution as well.

(ii) Note also that the boundedness of the asymptotic solution (4.6)–(4.8) for wide pulses ($W_0 > 2\sqrt{\epsilon}$) does not guarantee that the solution of the original equation (2.13) remains regular indefinitely. After all, the error of the asymptotic solution can accumulate and, after several cycles, still cause the disturbance to blow up. In fact, it might be possible that any initial disturbance governed by equation (2.13) blows up. This question requires further investigation.

5. The finite- q case

In this section, we shall briefly describe how the results obtained for the small- q limit can be generalized for the full equation (2.11). First, we study its harmonic solutions (using the WKB method), secondly, we examine this equation’s exploding solutions.

Substituting (3.1) for a harmonic solution into equation (2.11), we obtain

$$\frac{d}{d\theta} \left[C(\theta) \phi + \epsilon D(\theta) \sin \theta \frac{d\phi}{d\theta} \right] - i\omega B(\theta) \phi = 0, \tag{5.1}$$

where B , C and D are defined by (2.12)†. Equation (5.1) can be solved by the same WKB method that we used in the small- q limit. Omitting details, we present only the ‘final product’, i.e. the equation for the eigenfrequencies,

$$\int_0^{2\pi} \frac{\sqrt{C^2 - 4i\epsilon\omega BD \sin \theta} - C}{2\epsilon D \sin \theta} d\theta = 2\pi i n.$$

Just like its small- q equivalent (3.10), this equation has an infinite set of real roots and has no complex ones.

The generalization of the exploding solutions is a little less straightforward, mainly because the translation speed of disturbances is now variable (depends on θ). Generally, the speed of disturbances is determined by the ratio of the coefficients of $\partial h/\partial t$ and $\partial h/\partial \theta$ in the governing equation and, in the present case, is equal to

† Note that small terms in expressions (2.12) can be omitted, i.e. we can put $B=1$ and $C=1-\bar{h}^2 \cos \theta$. The simplified expressions, however, do not make our calculations any easier.

$C(\theta)/B(\theta)$. Accordingly, substitution (4.3) should be generalized as follows

$$x = \frac{\theta - \theta_p(t)}{\varepsilon^{1/2}},$$

where the current position of the pulse, θ_p , satisfies the following initial-value problem:

$$\frac{d\theta_p}{dt} = \frac{C(\theta_p)}{B(\theta_p)}, \quad \theta_p(0) = 0. \quad (5.2)$$

Equation (5.2) cannot be solved explicitly, of course, and $\theta_p(t)$ has to be treated as a 'general' function. Rewriting (2.11) in terms of (x, t) and keeping the leading-order terms only, we obtain

$$\frac{\partial h}{\partial t} = -F(t) \sin \theta \frac{\partial^2 h}{\partial x^2}, \quad (5.3)$$

where

$$F(t) = \frac{B^2(\theta_p)D(\theta_p)}{C^2(\theta_p)}. \quad (5.4)$$

Just like its small- q predecessor, equation (5.3) admits separation of variables,

$$h(x, t) = A(t) f(\xi), \quad (5.5)$$

where

$$\xi = \frac{x}{W(t)}.$$

Substituting (5.5) into (5.3), we solve the resulting equations for A , f and W . It turns out that the shape of the pulse and the relationship between the amplitude and width are exactly the same as those in the small- q limit,

$$f(\xi) = \exp(-\frac{1}{2}\xi^2), \quad A(t) = \frac{A_0 W_0}{W(t)}.$$

However, we can no longer find $W(t)$ explicitly,

$$W(t) = \sqrt{W_0^2 - 2\varepsilon \int_0^t F(t') \sin t' dt'}.$$

as this requires an explicit expression for $\theta_p(t)$ (see (5.4)). It can be readily shown, however, that, for sufficiently narrow pulses ($W_0 \rightarrow 0$), $W(t)$ vanishes for some $t = t_* \leq \pi$, and the solution blows up. The only difference between the general case and the small- q limit is that, for the former, we are unable to calculate explicitly the time of explosion and the threshold value of W_0 .

6. Summary and concluding remarks

In this paper, we described a hydrodynamic system with fairly unusual features:

(i) The system admits infinitely many harmonic solutions, all of which have real frequencies and are neutrally stable. (This result has been obtained using a modification of the WKB method, combined with the direct numerical integration of the corresponding eigenvalue problem – see §3).

(ii) On the other hand, the system admits (strongly unstable) solutions which develop singularities in a finite time (see §4).

In order to reconcile these two features, we assumed that the harmonic solutions form a complete set and that an arbitrary initial condition can be represented by an

expansion of those harmonics. Since the frequencies are real, each term of the series remains bounded for all $t > 0$, but the series as a whole may still diverge. The general conclusion to be drawn here is that harmonic solutions are not a completely reliable indicator of the stability properties of a system.

Observe, however, that equation (2.8) describing the exploding solutions has been derived from the exact equations using the lubrication approximation, which fails when the unstable solution is close to ‘explosion’. Thus, physically, our solutions describe only the initial stage of the instability, and it is unclear whether the exact solution exhibits any kind of singular behaviour.

We shall not discuss this question in detail, but mention only that the unstable (exploding) solutions found through the first-order approximation have a clear physical interpretation, and thus have a good chance of translating to the exact model. Indeed, imagine a short-scale perturbation on the surface of the film. When the rotation of the cylinder turns it ‘upside down’, gravity starts increasing its amplitude and/or shortening its size. Once the perturbation is sufficiently large and short, a drop of fluid can detach itself from the film and start falling down. Clearly, the exploding solution of the linear asymptotic equation describes the initial stage of this process, and, unless capillary effects are taken into account, the exact model should admit a similar solution as well. It would be interesting to confirm this physical argument by finding the exploding solution of the exact model.

Another possible extension of our results is associated with the proof of completeness of the harmonic solutions derived. Until now, we have only carried out numerical experiments with particular examples. In all cases, the truncation error decreased with the number of modes taken into account, which is a good indication of completeness. Another indication comes from the fact that our eigenfunctions, in a certain limit, tend to the set of complex exponentials, which do form a complete set (on which the complex Fourier series is based). Still, a formal proof of completeness would be preferable, even though obtaining it is a difficult task (mainly because the corresponding Sturm–Liouville operator is singular).

Finally, we note that instability of a liquid film in a rotating cylinder has been observed experimentally (e.g. Balmer 1970). It is, however, impossible, at this stage, to pinpoint whether the instability is caused by harmonic or explosive disturbances. Before a meaningful comparison with experimental data can be made, we must refine our model (by taking into account axial variability of the flow, surface tension, etc.).

The work was supported by Grant HEA PRLT1 (501-133-2889) and by the Institute for Nonlinear Science, Ireland.

Appendix A. Derivation of equation (2.8)

A two-dimensional flow of viscous fluid inside a cylinder with horizontal axis (see figure 1) is convenient to describe by the radial and angular velocities $u(r, \theta, t)$ and $v(r, \theta, t)$, and the pressure $p(r, \theta, t)$ (r and θ are polar coordinates, and t is the time). In terms of u , v and p , the governing equations are (e.g. Landau & Lifshitz 1995)

$$\frac{\partial u}{\partial t} + u \frac{\partial u}{\partial r} + \frac{v}{r} \left(\frac{\partial u}{\partial \theta} - v \right) + \frac{\partial p}{\partial r} = -g \sin \theta + v \left[\frac{1}{r} \frac{\partial}{\partial r} \left(r \frac{\partial u}{\partial r} \right) + \frac{1}{r^2} \left(\frac{\partial^2 u}{\partial \theta^2} - u - 2 \frac{\partial v}{\partial \theta} \right) \right],$$

(A 1)

$$\frac{\partial v}{\partial t} + u \frac{\partial v}{\partial r} + \frac{v}{r} \left(\frac{\partial v}{\partial \theta} + u \right) + \frac{1}{r} \frac{\partial p}{\partial \theta} = -g \cos \theta + \nu \left[\frac{1}{r} \frac{\partial}{\partial r} \left(r \frac{\partial v}{\partial r} \right) + \frac{1}{r^2} \left(\frac{\partial^2 v}{\partial \theta^2} - v + 2 \frac{\partial u}{\partial \theta} \right) \right], \quad (\text{A } 2)$$

$$\frac{\partial}{\partial r}(ru) + \frac{\partial v}{\partial \theta} = 0, \quad (\text{A } 3)$$

where g is the acceleration due to gravity and ν is the kinematic viscosity. We assume that the cylinder is rotating with constant angular velocity Ω , which corresponds to the following boundary condition:

$$u = 0, \quad v = \Omega R \quad \text{at } r = R, \quad (\text{A } 4)$$

where R is the radius of the cylinder. We also need boundary conditions on the free surface of the film, i.e. at $r = R - h(\theta, t)$, where h is the thickness of the film. We require that

$$\boldsymbol{\sigma} \mathbf{n} = \mathbf{0} \quad \text{at } r = R - h, \quad (\text{A } 5)$$

where

$$\mathbf{n} = \begin{bmatrix} 1 \\ \frac{1}{R-h} \frac{\partial h}{\partial \theta} \end{bmatrix}$$

is a vector normal to the surface, and

$$\boldsymbol{\sigma} = \begin{bmatrix} 2\nu \frac{\partial u}{\partial r} - p & \frac{\nu}{r} \left(\frac{\partial u}{\partial \theta} - v + r \frac{\partial v}{\partial r} \right) \\ \frac{\nu}{r} \left(\frac{\partial u}{\partial \theta} - v + r \frac{\partial v}{\partial r} \right) & \frac{2\nu}{r} \left(\frac{\partial v}{\partial \theta} + u \right) - p \end{bmatrix}$$

is the stress tensor (see Landau & Lifshitz 1995). Then, (A 5) yields

$$\left. \begin{aligned} 2\nu \frac{\partial u}{\partial r} - p + \frac{\nu}{(R-h)^2} \left[\frac{\partial u}{\partial \theta} - v + (R-h) \frac{\partial v}{\partial r} \right] \frac{\partial h}{\partial \theta} &= 0 \\ \nu \left[\frac{\partial u}{\partial \theta} - v + (R-h) \frac{\partial v}{\partial r} \right] + \left[\frac{2\nu}{R-h} \left(\frac{\partial v}{\partial \theta} + u \right) - p \right] \frac{\partial h}{\partial \theta} &= 0 \end{aligned} \right\} \quad \text{at } r = R - h. \quad (\text{A } 6)$$

We also require that the normal velocity of particles at the surface matches the normal velocity of the surface itself. A straightforward calculation yields

$$\frac{\partial h}{\partial t} + \frac{\nu}{R-h} \frac{\partial h}{\partial \theta} + u = 0 \quad \text{at } r = R - h.$$

This condition can be rewritten in a more convenient form. Integrate the continuity equation (A 3) with respect to r from $R - h$ to R and use the boundary condition for u (see (A 4)),

$$-[(R-h)u]_{r=R-h} + \frac{\partial}{\partial \theta} \int_{R-h}^R v \, dr - \frac{\partial h}{\partial \theta} v = 0.$$

Combining the last two equalities, we obtain

$$(R-h) \frac{\partial h}{\partial t} + \frac{\partial}{\partial \theta} \int_{R-h}^R v \, dr = 0. \quad (\text{A } 7)$$

As mentioned in the main body of the paper, the problem at hand is governed by three non-dimensional parameters, δ , G and N (defined by (2.1)–(2.3)). The lubrication

approximation corresponds to the assumptions $\delta \ll 1$ and $G \sim N \gg 1$, in which case the leading-order dynamics is determined by the pressure/gravity terms in (A 1), and the gravity/viscosity terms in (A 2). The corresponding non-dimensional variables are

$$\tilde{r} = \frac{1}{\delta} \frac{R-r}{R}, \quad \tilde{\theta} = \theta, \quad \tilde{t} = \Omega t, \quad (\text{A } 8)$$

$$\tilde{u} = \frac{1}{\delta} \frac{u}{R\Omega}, \quad \tilde{v} = \frac{v}{R\Omega}, \quad \tilde{p} = \frac{1}{\delta G} \frac{p}{(R\Omega)^2}, \quad \tilde{h} = \frac{1}{\delta} \frac{h}{R}. \quad (\text{A } 9)$$

We need to retain two orders of the lubrication expansion. At the same time, to keep calculations simple, we shall avoid taking into account the inertia terms. This can be achieved by properly choosing N and G , controlling to which extent the pressure/viscosity terms dominate the inertia terms. It can be verified by inspection that the proper choice is $N \sim G \sim \delta^{-2}$, or, equivalently,

$$N = \frac{N'}{\delta^2}, \quad G = \frac{G'}{\delta^2}, \quad (\text{A } 10)$$

where N' and G' are constants of order one.

Substituting (A 8)–(A 10) into the governing equations (A 1)–(A 7), we obtain (tildes omitted)

$$\begin{aligned} & \delta^2 \left[\delta \frac{\partial u}{\partial t} - \delta u \frac{\partial u}{\partial r} + \frac{v}{1-\delta r} \left(\delta \frac{\partial u}{\partial \theta} - v \right) \right] - G' \frac{\partial p}{\partial r} \\ & = -G' \sin \theta + N' \delta \left[\frac{\partial^2 u}{\partial r^2} - \frac{\delta}{1-\delta r} \frac{\partial u}{\partial r} + \frac{\delta}{(1-\delta r)^2} \left(\delta \frac{\partial^2 u}{\partial \theta^2} - \delta u - 2 \frac{\partial v}{\partial \theta} \right) \right], \quad (\text{A } 11) \end{aligned}$$

$$\begin{aligned} & \delta^2 \left[\frac{\partial v}{\partial t} - u \frac{\partial v}{\partial r} + \frac{v}{1-\delta r} \left(\frac{\partial v}{\partial \theta} + \delta u \right) \right] + \frac{G' \delta}{1-\delta r} \frac{\partial p}{\partial \theta} \\ & = -G' \cos \theta + N' \left[\frac{\partial^2 v}{\partial r^2} - \frac{\delta}{1-\delta r} \frac{\partial v}{\partial r} + \frac{\delta^2}{(1-\delta r)^2} \left(\frac{\partial^2 v}{\partial \theta^2} - v + 2\delta \frac{\partial u}{\partial \theta} \right) \right], \quad (\text{A } 12) \end{aligned}$$

$$-\frac{\partial}{\partial r} [(1-\delta r)u] + \frac{\partial v}{\partial \theta} = 0, \quad (\text{A } 13)$$

$$u = 0, \quad v = 1 \quad \text{at } r = 0, \quad (\text{A } 14)$$

$$\left. \begin{aligned} \frac{G'}{N'} p &= \left[\delta \left(\delta \frac{\partial u}{\partial \theta} - v \right) - (1-\delta h) \frac{\partial v}{\partial r} \right] \frac{\delta}{(1-\delta r)^2} \frac{\partial h}{\partial \theta} - 2\delta \frac{\partial u}{\partial r} \\ \frac{\partial v}{\partial r} &= \frac{\delta}{1-\delta h} \left(\delta \frac{\partial u}{\partial \theta} - v \right) + \frac{\delta}{1-\delta h} \left[\frac{2\delta}{1-\delta h} \left(\frac{\partial v}{\partial \theta} + \delta u \right) - \frac{G'}{N'} p \right] \frac{\partial h}{\partial \theta} \end{aligned} \right\} \quad \text{at } r = h, \quad (\text{A } 15)$$

$$(1-\delta h) \frac{\partial h}{\partial t} + \frac{\partial}{\partial \theta} \left(\int_0^h v \, dr \right) = 0. \quad (\text{A } 16)$$

Now, seek a solution of the form

$$u = u^{(0)} + \delta u^{(1)} + \dots \quad v = v^{(0)} + \delta v^{(1)} + \dots \quad p = p^{(0)} + \delta p^{(1)} + \dots$$

Our plan is as follows: using equations (A 11)–(A 15), we shall relate v to h and thus close equation (A 16).

In the leading order, (A 11)–(A 15) yield

$$\frac{\partial p^{(0)}}{\partial r} = \sin \theta, \quad \frac{\partial^2 v^{(0)}}{\partial r^2} = \frac{G'}{N'} \cos \theta, \quad \frac{\partial u^{(0)}}{\partial r} = \frac{\partial v^{(0)}}{\partial \theta}, \quad (\text{A } 17)$$

$$u^{(0)} = 0, \quad v^{(0)} = 1 \quad \text{at } r = 0, \quad (\text{A } 18)$$

$$p^{(0)} = 0, \quad \frac{\partial v^{(0)}}{\partial r} = 0 \quad \text{at } r = h. \quad (\text{A } 19)$$

Solving (A 17)–(A 19), we obtain

$$p^{(0)} = (r - h) \sin \theta, \quad u^{(0)} = \frac{G'}{N'} \left[\left(\frac{1}{2} r^2 h - \frac{1}{6} r^3 \right) \sin \theta - \frac{1}{2} r^2 h_\theta \cos \theta \right],$$

$$v^{(0)} = 1 + \frac{G'}{N'} \left(\frac{1}{2} r^2 - rh \right) \cos \theta. \quad (\text{A } 20)$$

In the next order, we need only the equation and boundary conditions for $v^{(1)}$,

$$\frac{\partial^2 v^{(1)}}{\partial r^2} = \frac{\partial v^{(0)}}{\partial r} + \frac{G'}{N'} \frac{\partial p^{(0)}}{\partial \theta}, \quad (\text{A } 21)$$

$$v^{(1)} = 0 \quad \text{at } r = 0, \quad (\text{A } 22)$$

$$\frac{\partial v^{(1)}}{\partial r} = -v^{(0)} - \frac{G'}{N'} p^{(0)} \frac{\partial h}{\partial \theta} \quad \text{at } r = h. \quad (\text{A } 23)$$

The solution to (A 21)–(A 23) is

$$v^{(1)} = -r + \frac{G'}{N'} \left[\left(\frac{1}{3} r^3 - r^2 h + \frac{3}{2} r h^2 \right) \cos \theta + \left(rh - \frac{1}{2} r^2 \right) \frac{\partial h}{\partial \theta} \sin \theta \right]. \quad (\text{A } 24)$$

Summarizing (A 20) and (A 24), we obtain

$$v = 1 + \frac{G'}{N'} \left(\frac{1}{2} r^2 - rh \right) \cos \theta + \delta \left\{ -r + \frac{G'}{N'} \left[\left(\frac{1}{3} r^3 - r^2 h + \frac{3}{2} r h^2 \right) \cos \theta + \left(rh - \frac{1}{2} r^2 \right) \frac{\partial h}{\partial \theta} \sin \theta \right] \right\} + O(\delta^2). \quad (\text{A } 25)$$

Substitution of (A 25) into (A 16) yields

$$(1 - \delta h) \frac{\partial h}{\partial t} + \frac{\partial}{\partial \theta} \left\{ h - \frac{G'}{N'} \frac{1}{3} h^3 \cos \theta + \frac{\partial}{\partial \theta} \delta \left[-\frac{1}{2} h^2 + \frac{G'}{N'} \left(\frac{1}{2} h^4 \cos \theta + \frac{1}{3} h^3 h_\theta \sin \theta \right) \right] \right\} = O(\delta^2). \quad (\text{A } 26)$$

We note that the expression in curly brackets (the mass flux) coincides with the corresponding expression derived by Johnson (1988).

Rewriting (A 26) in terms of

$$\hat{\theta} = \theta, \quad \hat{t} = t, \quad \hat{h} = \sqrt{\frac{G'}{N'}} h.$$

omitting the hats, and introducing

$$\varepsilon = \delta \sqrt{\frac{N'}{G'}},$$

we obtain

$$(1 - \epsilon h) \frac{\partial h}{\partial t} + \frac{\partial}{\partial \theta} \left[h - \frac{1}{3} h^3 \cos \theta + \epsilon \left(-\frac{1}{2} h^2 + \frac{1}{2} h^4 \cos \theta + \frac{1}{3} h^3 h_\theta \sin \theta \right) \right] = O(\epsilon^2). \quad (\text{A } 27)$$

which differs from (2.8) only by the unspecified small terms on the right-hand side.

Finally, observe that (A 27) (and hence (2.8)) can be reduced to a slightly simpler equation by changing to a new variable,

$$\eta = h - \frac{1}{2} \epsilon h^2.$$

Reversing this equality, we obtain

$$h = \eta + \frac{1}{2} \epsilon \eta^2 + O(\epsilon^2). \quad (\text{A } 28)$$

Substitution of (A 28) into (A 27) yields

$$\frac{\partial \eta}{\partial t} + \frac{\partial}{\partial \theta} \left(\eta - \frac{1}{3} \eta^3 \cos \theta + \frac{1}{3} \epsilon \eta^3 \frac{\partial \eta}{\partial \theta} \sin \theta \right) = O(\epsilon^2). \quad (\text{A } 29)$$

It should be emphasized that equations (A 27) and (A 29) are not equivalent, but asymptotically equivalent (they differ by $O(\epsilon^2)$ terms).

Despite the relative simplicity of (A 29), we shall use (A 27), as the latter is written in terms of the ‘natural’ variable h . The former, however, should be useful for numerical simulations, as it allows us to significantly reduce the number of operations per time step.

Appendix B. Singular points of equation (3.2)

Observe that $\theta = 0$ and $\theta = \pi$ are singular points of equation (3.2), as the coefficient of the highest-order derivative at these points vanish. In order to understand the implications of the singularities, consider first $\theta = 0$. In the vicinity of this point, equation (3.2) has two linearly independent solutions, the expansions of which can be readily obtained using the Frobenius method†,

$$\phi_1 = 1 + \frac{i\omega}{\epsilon + 1} \theta + \dots \quad \phi_2 = |\theta|^{-1/\epsilon} \left[1 + \frac{i\omega}{\epsilon - 1} \theta + \dots \right] \quad \text{as } \theta \rightarrow 0. \quad (\text{B } 1)$$

Note that, owing to the singularity, the ‘weights’ of ϕ_1 and ϕ_2 in the solution ϕ do not have to be the same to the right and to the left of $\theta = 0$, i.e.

$$\phi = a_1^{(+)} \phi_1 + a_2^{(+)} \phi_2 \quad \text{as } \theta \rightarrow +0,$$

$$\phi = a_1^{(-)} \phi_1 + a_2^{(-)} \phi_2 \quad \text{as } \theta \rightarrow -0,$$

where $a_{1,2}^{(+)}$ and $a_{1,2}^{(-)}$ are (possibly different) constants, which cannot be calculated from equation (3.2).

In order to determine $a_{1,2}^{(+)}$ and $a_{1,2}^{(-)}$, an ‘external’ physical constraint should be imposed. We require that the thickness of the film and the mass flux be continuous

† Observe that one of the following expansions is invalid if $\epsilon = 1$. An explanation of how this can be corrected can be found in Appendix C. This question is of limited importance, as, physically, ϵ is a small parameter.

functions, i.e.

$$\phi \quad \text{is continuous for all } \theta, \tag{B 2}$$

$$\phi + \epsilon \sin \theta \frac{d\phi}{d\theta} \quad \text{is continuous for all } \theta. \tag{B 3}$$

Since ϕ_2 is singular as $\theta \rightarrow \pm 0$, it satisfies neither (B 2) nor (B 3) – hence, $a_2^{(\pm)} = 0$. ϕ_1 , in turn, is regular, and (B 2)–(B 3) yield $a_1^{(+)} = a_2^{(-)}$. Thus, ϕ is regular at $\theta = 0$.

For the second singular point, $\theta = \pi$, we have

$$\phi = b_1^{(+)}\psi_1 + b_2^{(+)}\psi_2 \quad \text{as } \theta \rightarrow \pi + 0,$$

$$\phi = b_1^{(-)}\psi_1 + b_2^{(-)}\psi_2 \quad \text{as } \theta \rightarrow \pi - 0,$$

where $b_{1,2}^{(\pm)}$ are constants, and the linearly independent solutions are

$$\psi_1 = 1 + \frac{i\omega}{\epsilon - 1}(\theta - \pi) + \dots \quad \psi_2 = |\theta - \pi|^{1/\epsilon} \left[1 + \frac{i\omega}{\epsilon + 1}(\theta - \pi) + \dots \right] \quad \text{as } \theta \rightarrow \pi. \tag{B 4}$$

Unlike the previous case, the second solution is now finite; moreover, ψ_2 ‘produces’ zero values of the film thickness and mass flux as $\theta \rightarrow \pi$. Hence, (B 2)–(B 3) hold for any values of $b_2^{(\pm)}$, and we conclude that these coefficients should remain unrestricted (in fact, any constraint imposed on $b_2^{(\pm)}$ makes the problem overdetermined). We need only to match the coefficients of ψ_1 , for which (B 2)–(B 3) yield $b_1^{(+)} = b_1^{(-)}$. In other words, we can simply require that ϕ be continuous at $\theta = \pi$.

Appendix C. The numerical method for the eigenvalue problem (3.2), (3.3)

Boundary-value problems with infinite number of eigenvalues are usually solved by reducing them to an eigenvalue problem for a matrix. In application to (3.2), (3.3), the simplest method would probably be based on representing the solution by its complex Fourier series,

$$\phi(\theta) = \sum_{k=-\infty}^{\infty} m_k e^{ik\theta}, \tag{C 1}$$

where m_k are the Fourier coefficients. Representation (C 1) automatically satisfies both boundary conditions (regularity at $\theta = 0$ and periodicity), hence, we need to satisfy only equation (3.2). Upon substitution of (C 1) into (3.2), the problem reduces to finding the eigenvalues of an infinite tri-diagonal matrix (the eigenvectors of this matrix are made up of m_k). Truncating the eigenvectors and matrix at a large, but finite $k = \pm K$, we can find the eigenvalues through one of the standard methods available, say, in the MATLAB package.

It turned out, however, that the truncation error is extremely large for the problem at hand and makes this algorithm simply impossible to use. For example, for $K = 1000$, the number of reliably computed eigenvalues is only about 20 (10 positive and 10 negative†).

In order to clarify why this occurs, we represent equation (3.2) in the form $\mathcal{L}\phi = \omega\phi$, where

$$\mathcal{L} = i\epsilon \sin \theta \frac{d^2}{d\theta^2} + i(1 + \epsilon \cos \theta) \frac{d}{d\theta}, \tag{C 2}$$

† It can be readily shown that, if ω is an eigenvalue of (3.2), (3.3), then $-\omega$ is also an eigenvalue.

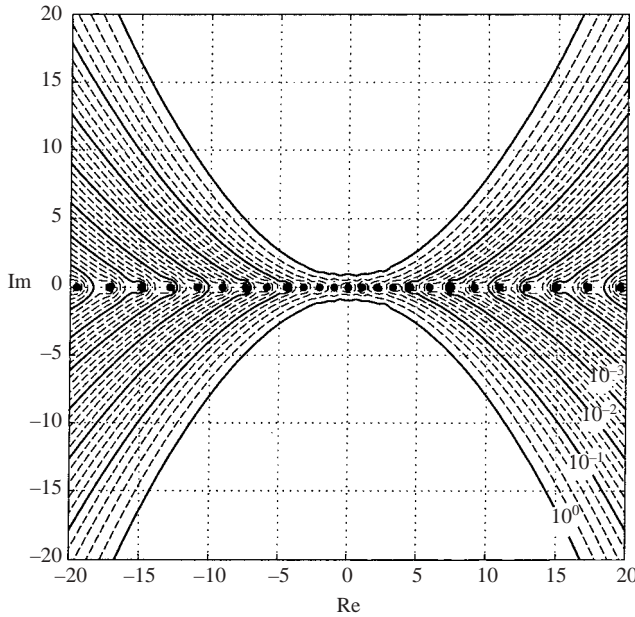


FIGURE 6. The pseudospectra of the operator \mathcal{L} (defined by (C2)).

and calculate the so-called pseudospectrum of \mathcal{L} (Trefethen *et al.* 1993),

$$\Lambda_\eta = \{ \omega : \| \mathcal{L} - \omega \mathcal{I} \| < \eta \},$$

where \mathcal{I} is the unit operator. As follows from the definition, the eigenvalues of \mathcal{L} are represented by Λ_0 , whereas, for finite η , Λ_η can be interpreted as the set of points which ‘miss’ one of the eigenvalues by a value of η . The pseudospectrum of \mathcal{L} is shown in figure 6 – we can see that $\| \mathcal{L} - \omega \mathcal{I} \|$ rapidly decays as $\text{Im } \omega \rightarrow \pm\infty$. As a result, truncation of the solution’s Fourier expansion can dramatically change the computed positions of large eigenvalues†.

Alternatively, the eigenvalue problem (3.2), (3.3) can be solved using the shooting method. This was not a straightforward task, with the main difficulty being created by the singularities at $\theta = 0, \pi$. The solution cannot be computed near these points, and we represented it analytically by Frobenius expansions. Even this approach has its share of problems, as the convergence radius of the series turned out to vanish as $\epsilon \rightarrow 0$ (which is the most interesting limit). As a result, we had to take into account as many as 10 terms of the expansion (for the higher modes). Another difficulty arose if ϵ was a reciprocal of an integer (for example, $\epsilon = 0.1$). In such cases, the Frobenius expansion for equation (3.2) includes logarithmic terms, which make the calculations particularly cumbersome. Eventually, the calculation of the coefficients of the series was carried out using the MAPLE package.

† It is also worth noting that, unlike previously known cases, the pseudospectra of \mathcal{L} appear to reach infinitely large values of $\text{Im } \omega$ (instead of peaking out at a finite value of $\text{Im } \omega$ and going back to the real axis). This is another indication that growth of disturbances in the present problem is particularly strong.

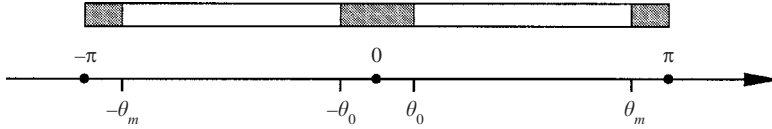


FIGURE 7. The subdivision of the computational domain. The singular points of equation (3.2) are shown by dots, and the matching points are shown by ticks. The subdomains where the solution was computed using its Frobenius expansion are shaded.

Our numerical algorithm involved the following steps:

(i) The computational domain, $-\pi < \theta < \pi$, was divided into 5 subdomains: $(-\pi, -\theta_m)$, $(-\theta_m, -\theta_0)$, $(-\theta_0, \theta_0)$, (θ_0, θ_m) and (θ_m, π) (see figure 7). θ_0 was chosen near 0, and θ_m near π .

(ii) In the subdomain $(-\theta_0, \theta_0)$, the solution was computed using the Frobenius expansion of ϕ_1 (defined by (B 1)). The second particular solution, ϕ_2 , was discarded, as it is inconsistent with conditions (B 2)–(B 3).

(iii) In the subdomains $(-\theta_m, -\theta_0)$ and (θ_0, θ_m) , the solution was computed using the MATLAB's algorithm ODE23S (an algorithm with adjustable step, designed for stiff problems).

(iv) In the subdomains $(-\pi, -\theta_m)$ and (θ_m, π) , the solution was computed using the Frobenius expansions. Both particular solutions, ψ_1 and ψ_2 (defined by (B 4)) were taken into account. To determine the 'weights' of ψ_1 and ψ_2 , the solution and its derivative were matched at $\theta = \pm\theta_m$ to those in the subdomains $(-\theta_m, -\theta_0)$ and (θ_0, θ_m) .

(v) Finally, the value of $\phi(\pi) - \phi(-\pi)$ was fed into a root-finding routine based on the secant method, which determined ω .

The above algorithm turned out to be highly sensitive to the choice of θ_m (which needs to be carefully adjusted), whereas the dependence on θ_0 is much more robust.

REFERENCES

- BALMER, R. T. 1970 The hydrocyst: a stability phenomenon in continuum mechanics. *Nature* **227**, 600–601.
- BLOMBERGEN, N. 1965 *Nonlinear Optics*. Benjamin, New York.
- CHAPMAN, S. J. 2002 Subcritical transition in channel flow. *J. Fluid Mech.* **451**, 35–97.
- DRAZIN, P. G. & REID, W. H. 1981 *Hydrodynamic Stability*. Cambridge University Press.
- FARREL, B. F. 1982 Modal and nonmodal baroclinic waves. *J. Atmos. Sci.* **41**, 1663–1686.
- JOHNSON, R. E. 1988 Steady state coating flows inside a rotating horizontal cylinder. *J. Fluid Mech.* **190**, 321–342.
- LANDAU, L. & LIFSHITZ, E. 1995 *Course of Theoretical Physics, vol. 6: Fluid Mechanics*. Pergamon.
- MOFFAT, H. K. 1977 Behaviour of a viscous film on the outer surface of a rotating cylinder. *J. Méc.* **16**, 651–674.
- O'BRIEN, S. B. G. 2002a Linear stability of rimming flows. *Q. Appl. Maths* **60**, 201–212.
- O'BRIEN, S. B. G. 2002b A mechanism for two dimensional instabilities in rimming flow. *Q. Appl. Maths.* **60**, 283–300.
- O'BRIEN, S. B. G. & GATH, E. G. 1998 The location of a shock in rimming flow. *Phys. Fluids* **10**, 1040–1042.
- SAZONOV, I. A. 1996 Evolution of three-dimensional wave packets in the Couette flow. *Izv. RAN, Atmos. Ocean Phys.* **32**, 27–34.
- TREFETHEN, L. N., TREFETHEN, A. E., REDDY, S. C. & DRISCOLL, T. A. 1993 Hydrodynamic stability without eigenvalues. *Science* **261**, 578–584.